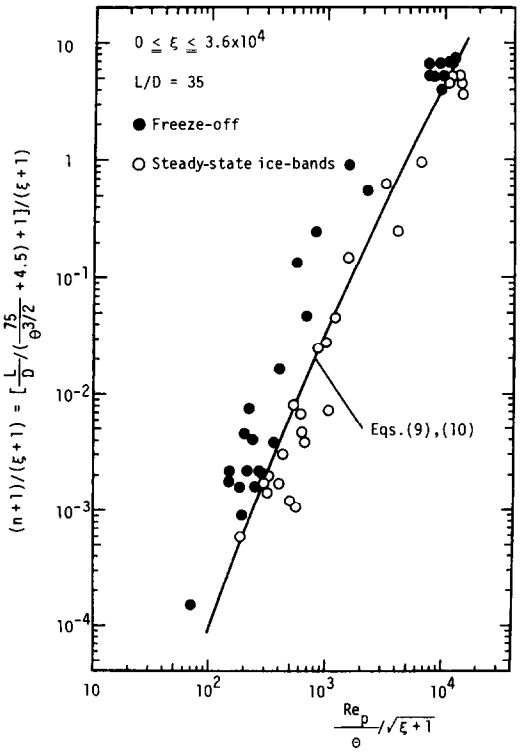

FIG. 3. A correlation of the freeze-off conditions for a wide range of ξ.

factor coefficient, $0 \leqslant \xi \leqslant 3.6 \times 10^4$. The upper region of the predicted line shows a freeze-off regime and the lower, a steady-state ice-band. Taking into account that the morphology of the ice layer under which the experimental conditions are close to the onset of freeze-off is often affected by small disturbances in temperature and flow conditions, it can be said that equations (9) and (10) give good predictions for the effects of the friction-factor on the freeze-off conditions.

CONCLUDING REMARKS

The onset of freeze-off was examined for the case that the friction-factor coefficient, ξ, in water-flow pipe systems was dominant. It has been ascertained both experimentally and analytically that the freeze-off easily occurs for a larger value of ξ and the effect of ξ on the freeze-off conditions can be given by equations (9) and (10).

REFERENCES

1. R. R. Gilpin, T. Hirata and K. C. Cheng, Wave formation and heat transfer at an ice-water interface in the presence of a turbulent flow, *J. Fluid Mech.* **99,** 619–640 (1980).
2. R. R. Gilpin, The morphology of ice structure in a pipe at or near transition Reynolds numbers, *A.I.Ch.E. Symp. Ser.* **75,** 89–94 (1979).
3. R. R. Gilpin, Ice formation in a pipe containing flows in the transition and turbulent regimes, *J. Heat Transfer* **103,** 363–368 (1981).
4. T. Hirata and M. Ishihara, Freeze-off conditions of a pipe containing a flow of water, *Int. J. Heat Mass Transfer* **28,** 331–337 (1985).

Int. J. Heat Mass Transfer. Vol. 29, No. 6, pp. 951–954, 1986
Printed in Great Britain

0017–9310/86 $3.00 + 0.00
Pergamon Journals Ltd.

Boundary-layer treatment of film condensation in the presence of a solid matrix

M. KAVIANY
Department of Mechanical Engineering and Applied Mechanics, University of Michigan, Ann Arbor, MI 48109, U.S.A.

(*Received* 23 *July* 1985 *and in final form* 8 *November* 1985)

1. INTRODUCTION

LAMINAR, steady-state film condensation and boiling, along a plane surface submerged in a porous medium, have been studied analytically [1, 2] assuming that capillarity and non-Darcian effects are not significant.

The results, based on these assumptions, give the Nusselt number, condensate flow rate, and film thickness as a function of the subcooling (or superheating) parameter. The Prandtl number, which is introduced through the comparison between the thermal and momentum boundary-layer thickness, is not present because of the uniform film velocity distribution resulting from the application of Darcy's law. The capillary pressure, which is proportional to $\sigma(K/\varepsilon)^{-1/2}$ and depends on the saturation, can become significant at low permeabilities.

As the permeability increases, the inertia and boundary effects become important and for very high permeabilities the results based on no rigid matrix present [3, 4] must hold. However, since the film thickness decreases with an increase in permeability, then for the boundary-layer treatment to be valid, the small length scale associated with the microstructure of the rigid matrix must be much smaller than the film thickness. If this condition is satisfied, then the non-Darcy regime can be examined and, also, the parameters indicative of transition to the Darcian regime can be determined.

In this study the boundary layer and similarity treatment of film condensation in the absence of any solid matrix [3, 4] are extended to include the first-order resistance resulting from the presence of a solid matrix. This is done by applying an expansion method [5] (up to a third order) which has previously been used for treating natural convection in porous media [6]. The findings are then compared to those based on application of Darcy's law [1, 2].

NOMENCLATURE

c	$[g\Delta\rho(4\rho_l\nu_l^2)^{-1}]^{1/4}$
c_p	specific heat capacity [kJ kg^{-1} K^{-1}]
f	streamfunction defined by equation (6)
Gr_x	Grashof number, $g\Delta\rho x^3\rho_l^{-1}\nu_l^{-2}$; also called Archimedes number, Ar_x
h_{fg}	heat of evaporation [kJ kg^{-1}]
k_e	effective thermal conductivity [W m^{-1} K^{-1}]
K	permeability [m^2]
Nu_x	Nusselt number, $qx(T_w-T_s)^{-1}k_e^{-1}$
T	temperature [K]
ΔT	T_w-T_s [K]
Pr	Prandtl number, $\alpha_e\nu_l^{-1}$
u, v	velocity components, along and perpendicular to the plate [m s^{-1}]
x, y	coordinate axes, along and perpendicular to the plate [m].

Greek symbols

α_e	effective thermal diffusivity [m^2 s^{-1}]
δ	film thickness [m]
γ_x	porous media shape parameter, $(\varepsilon x^2K^{-1})^{1/2}$
ε	porosity
η	similarity variable, $cyx^{-1/4}$
θ	$(T-T_s)/(T_w-T_s)$
ν	kinematic viscosity [m^2 s^{-1}]
ξ_x	expansion parameter, $\varepsilon x^{1/2}c^{-2}K^{-1}=2\gamma_x^2Gr_x^{-1/2}$
ρ	density [kg m^{-3}]
$\Delta\rho$	$\rho_l-\rho_v$ [kg m^{-3}]
σ	surface tension [N m^{-1}]
ψ	streamfunction
Γ	condensate mass flow rate [kg m^{-1} s^{-1}]
Δ	nondimensional film thickness, $c\delta x^{-1/4}$.

Subscripts

e	effective
l	liquid
s	saturation
w	wall
v	vapor.

2. ANALYSIS

When no rigid matrix is present the condensate flow rate and other quantities of interest depend on the Prandtl number, Pr, and the extent of subcooling, $c_p\Delta T/h_{fg}$. For higher Prandtl numbers the convective term in the energy equation becomes insignificant; therefore, the results are independent of the Prandtl number, as are the results obtained based on Darcy's law [1, 2]. For a two-dimensional boundary-layer flow with a first-order resistance due to the presence of a rigid matrix, we have

$$\frac{\partial u}{\partial x}+\frac{\partial v}{\partial y}=0, \tag{1}$$

$$\rho_l u\frac{\partial u}{\partial x}+\rho_l v\frac{\partial u}{\partial y}=\mu_l\frac{\partial^2 u}{\partial y^2}-K^{-1}\varepsilon\mu_l u-g(\rho_l-\rho_v), \tag{2}$$

$$u\frac{\partial T}{\partial x}+v\frac{\partial T}{\partial y}=\alpha_e\frac{\partial^2 T}{\partial y^2}. \tag{3}$$

The boundary conditions are:

$$\begin{aligned} T&=T_w && \text{at} \quad y=0\\ T&=T_s && \text{at} \quad y=\delta\\ T&=T_s && \text{at} \quad x=0\\ u&=v=0 && \text{at} \quad y=0\\ u_y&=0 && \text{at} \quad y=\delta\\ u&=v=0 && \text{at} \quad x=0. \end{aligned}$$

The interfacial shear, which is significant for low Prandtl numbers [4], has been neglected.

In addition, an overall energy balance yields

$$\int_0^x k_e\frac{\partial T}{\partial y}\bigg|_0 dx=\int_0^\delta \rho_l h_{fg}u\,dy+\int_0^\delta \rho_l c_p u(T_s-T)\,dy. \tag{4}$$

In the following approximate solutions to equations (1)–(4) are found for cases where the flow field is not severely altered due to the presence of the solid matrix. This is done by making an expansion about the solution for the case where no rigid matrix is present. The method is similar to that used in [5] for inclusion of blowing or suction.

Equations (2) and (3) are scaled using $\eta=cyx^{-1/4}$ and a perturbation parameter

$$\xi_x=c^{-2}K^{-1}\varepsilon x^{1/2}=2\gamma_x^2Gr_x^{-1/2} \tag{5}$$

where $Gr_x=g(\rho_l-\rho_v)x^3\ (\rho_l\nu_l^2)^{-1}$ is the Grashof or Archimedes number, and $\gamma_x^2=\varepsilon x^2K^{-1}$ is the porous media shape parameter. Note that when $K\to\infty$, then $\xi_x=0$ and η becomes the only independent variable. The streamfunction can be defined as

$$\psi=4\nu_l cx^{3/4}f, \tag{6}$$

where

$$c^4=Gr_x/4. \tag{7}$$

Based on these substitutions the velocity components are

$$u=4\nu_l c^2x^{1/2}\frac{\partial f}{\partial\eta}$$

and

$$v=-4\nu_l cx^{-1/4}\left(\frac{3}{4}f-\frac{\eta}{4}\frac{\partial f}{\partial\eta}+\frac{\xi}{2}\frac{\partial f}{\partial\xi}\right),$$

and equations (2) and (3) become

$$f_{\eta\eta\eta}+3ff_{\eta\eta}-2f_\eta^2+2\xi[f_\eta(-\tfrac{1}{2}-f_{\eta\xi})+f_\xi f_{\eta\eta}]=-1 \tag{2a}$$

and

$$Pr^{-1}T_{\eta\eta}+\theta_\eta(3f+2\xi f_\xi)-2\xi\theta_\xi f_\eta=0, \tag{3a}$$

where the subscripts indicate partial differentiation.

Now, we assume the following expansion

$$f=\sum_{i=0}^{\infty}\xi_x^i f_i,\quad f_i=f_i(\eta),\quad i=1,2,3$$

$$\theta=\sum_{i=0}^{\infty}\xi_x^i\theta_i,\quad \theta_i=\theta_i(\eta).$$

The differential equations emerging from these substitutions are given in [6] where f_0 and T_0 are the available solutions for the case of no solid matrix present [3, 4].

Based on the energy equation and after transformation and

differentiation of equation (4), we have

$$-3\left[\sum_{i=0}^{\infty}\xi_x^i f_i(\Delta)\right]\Big/\left[\sum_{i=0}^{\infty}\xi_x^i\theta_i'(\Delta)\right]=\frac{c_p\Delta T}{h_{fg}}. \quad (4a)$$

In general, given Pr and $c_p\Delta T/h_{fg}$ (called the Kutateladze number, Ku), the dimensionless film thickness, Δ, the local Nusselt number, Nu_x, and the condensate flow rate, Γ/μ_l can be determined. The film thickness is implicitly obtained from equation (4a) and the local Nusselt number and the condensate flow rate are

$$\frac{2^{1/2}Nu_x}{Gr_x^{1/4}}=-\sum_{i=0}^{\infty}\xi_x^i\theta_i'(0), \quad (8)$$

$$\frac{\Gamma}{2^{3/2}Gr_x^{1/4}\mu_l}=\sum_{i=0}^{\infty}\xi_x^i f_i(\Delta). \quad (9)$$

The standard numerical technique used in the integration of the initial value problems was applied to the equations emerging from the expansion (these equations are given in ref. [6] except for the driving force which is a constant equal to unity and is present only for the zeroth-order equation) and the desired derivatives were determined for i up to 3. Some examples of the results are given in Table 1. Complete agreement has been found for $i=0$ by comparison with results given in refs. [3, 4]. Note that the interfacial shear stress was not included in this study. The range of ξ_x for which equations (8) and (9) are applicable will be discussed in the next section.

For Darcian flow, i.e. for large ξ_x, we have [1]

$$\frac{2^{1/2}Nu_x}{Gr_x^{1/4}}=\frac{2}{\pi^{1/2}}\{Pr/[\xi_x\,\mathrm{erf}\,(\Delta\xi_x^{-1/2}Pr^{1/2})]\}^{1/2}, \quad (10)$$

$$\frac{h_{fg}}{2c_p\Delta T}+\frac{1}{\pi}=1/\{\pi[\mathrm{erf}\,(\Delta\xi_x^{-1/2}Pr^{1/2})]^2\}, \quad (11)$$

and

$$\frac{\Gamma}{2^{3/2}Gr_x^{1/4}\mu_l}=\xi_x^{-1}\Delta. \quad (12)$$

3. RESULTS AND DISCUSSION

The Prandtl number influences the film thickness through the convection term in the energy equation [equation (3a)], and for relatively low Prandtl numbers the temperature profile becomes nearly linear. On the other hand, the film thickness increases monotonically with $c_p\Delta T/h_{fg}$.

For a given Pr and $c_p\Delta T/h_{fg}$, one is interested in (1) the effect of the resistance due to the presence of a solid matrix, and (2) the effect of the non-Darcian terms on the film thickness and other quantities. Here it is evident that: (a) as the resistance increases the average film velocity decreases and the film thickness increases as shown in refs. [1, 2], and (b) since Darcy's law does not allow for no-slip at the wall, its application leads to a smaller film thickness than that for no-slip. Similarly, the absence of the inertia (development) term results in higher velocities. Therefore, for high permeabilities, when the non-Darcy effects become significant, equation (11) underpredicts the film thickness.

Figure 1 shows the results for $Pr=0.03$ and 10. The similarity solution from ref. [1], i.e. equation (11), as well as the solutions obtained here by the expansion method, are given. The results show that the extent of the non-Darcy regime increases with a decrease in $c_p\Delta T/h_{fg}$. Table 2 gives some typical results for foams as the rigid matrix and mercury as the fluid. Consider the non-Darcy regime for a film thickness of 1–3 mm and $Pr=0.03$. If the small length scale is taken as $(K/\varepsilon)^{1/2}$, then for $K=10^{-7}$ m^2 this is 0.3 mm. Since the film thickness is not much larger than the pore size, the results are not very meaningful. For $\xi_x>100$ the results based on Darcy's law, i.e. equations (10)–(12), hold. For water the film

Table 1. Solutions to the similarity equations

Pr	Δ	$f_0''(0)$	$f_0'(\Delta)$	$f_0(\Delta)$	$\theta_0'(0)$	$\theta_0(\Delta)$	$f_1''(0)$	$f_1'(\Delta)$	$f_1(\Delta)$	$\theta_1'(0)$	$\theta_1(\Delta)$
0.03	1.8	0.1057E+1	0.6695E+0	0.8912E+0	−0.5643E+0	−0.5330E+0	−0.2578E+0	−0.1713E+0	−0.2378E+0	0.3930E−2	−0.9954E−2
	1.2	0.9645E+0	0.5118E+0	0.4248E+0	−0.8372E+0	−0.8228E+0	−0.2228E+0	−0.1378E+0	−0.1136E+0	0.1714E−2	−0.4664E−2
	0.8	0.7531E+0	0.2920E+0	0.1572E+0	−0.1251E+1	−0.1246E+1	−0.1270E+0	−0.6052E−1	−0.3152E−1	0.4564E−3	−0.1278E−2
	0.5	0.4949E+0	0.1231E+0	0.4109E−1	−0.2000E+1	−0.1999E+1	−0.3952E−1	−0.1225E−1	−0.3931E−2	—	—
10	0.3	0.2996E+0	0.4491E+0	0.8930E−2	−0.3360E+1	−0.3260E+1	−0.8937E−2	−0.1674E−2	−0.3215E−3	0.1518E−2	−0.4234E−2
Pr	Δ	$f_2''(0)$	$f_2'(\Delta)$	$f_2(\Delta)$	$\theta_2'(0)$	$\theta_2(\Delta)$	$f_3''(0)$	$f_3'(\Delta)$	$f_3(\Delta)$	$\theta_3'(0)$	$\theta_3(\Delta)$
0.03	1.8	0.3687E−1	0.1191E−1	0.2267E−1	−0.6260E−3	0.1370E−2	−0.7209E−3	0.1636E−2	0.1631E−2	−0.2520E−3	0.4679E−3
	1.2	0.3644E−1	0.1800E−1	0.1628E−1	−0.3651E−3	0.9534E−3	−0.1931E−2	0.2768E−3	−0.2021E−3	0.1287E−4	0.5091E−4
	0.8	0.2071E−1	0.9544E−2	0.5047E−2	−0.1031E−3	0.2870E−3	−0.2431E−2	−0.1002E−2	−0.5535E−3	—	—
	0.5	0.3630E−2	0.1136E−3	0.3638E−3	—	—	−0.3177E−3	−0.9647E−4	−0.3166E−4	—	—
10	0.3	0.3181E−3	0.6051E−4	0.1157E−4	−0.7519E−4	0.2092E−3	−0.0136E−4	−0.2163E−5	−0.4136E−6	0.3397E−5	−0.9497E−5

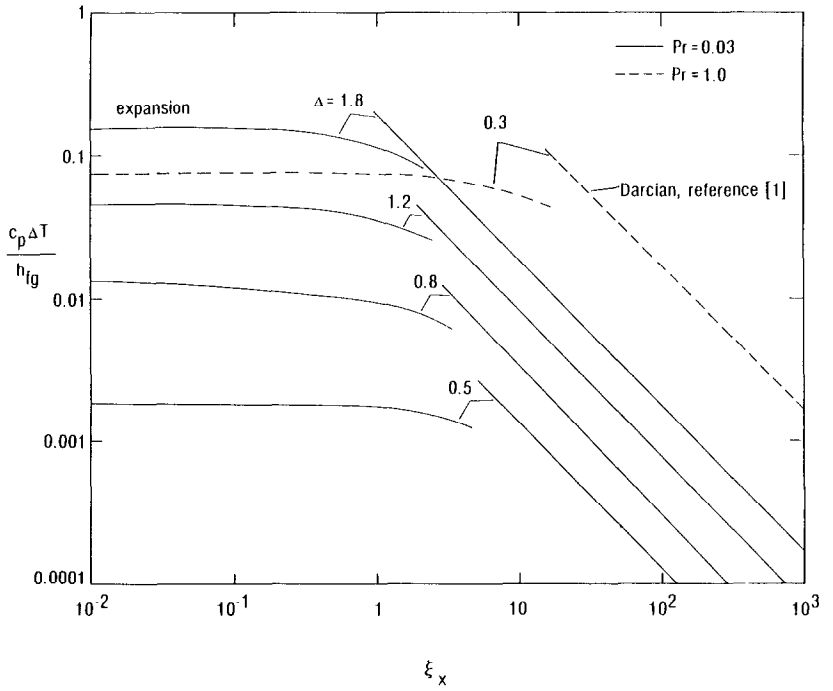

FIG. 1. Comparison of the results obtained by the third-order expansion and those based on Darcy's law, $Pr = 0.03$ and 10.

Table 2. Film thickness for two different fluids and some foams

Fluid			Geometry			Primary dimensionless variables					Range of film thickness	Regime*
$g\Delta\rho/\rho_l\nu_l^2$ (m^{-3})	c_p/h_{fg} ($°C^{-1}$)	ΔT (°C)	K (m^2)	ε	x (m)	Gr_x	γ_x^2	Pr_c	$c_p\Delta T/h_{fg}$	ξ_x	δ (mm)	
10^{11} (mercury)	5×10^{-4}	2–300	10^{-6}	0.9	0.1	10^8	10^4	0.03	0.001–0.15	2	1–3	Non-Darcian
			10^{-8}				10^6			2×10^2	3–40	Darcian
			10^{-10}				10^8			2×10^4	30–400	Darcian
10^{13} (water)	2×10^{-3}	2–100	10^{-6}			10^{10}	10^4	10	0.004–0.2	0.2	0.1–0.2	Non-Darcian
			10^{-8}				10^6			20	0.1–0.8	Non-Darcian
			10^{-10}				10^8			2×10^3	1–8	Darcian

* Based on extrapolation, and also analogy with the results for natural convection.

thickness is smaller but the non-Darcy effects persist even for lower permeabilities.

The results given in Figure 1 allow an approximation of the value of ξ_x above which the non-Darcian effects become significant, i.e. the limit of applicability of equations (10)–(12). This transitional ξ_x depends on the Prandtl number and increases as Pr increases, which is similar to the results found for natural convection [6]).

REFERENCES

1. P. Cheng, Film condensation along an inclined surface in a porous medium, *Int. J. Heat Mass Transfer* **24,** 983–990 (1981).
2. E. M. Parmentier, Two-phase natural convection adjacent to a vertical heated surface, *Int. J. Heat Mass Transfer* **22,** 849–855 (1979).
3. E. M. Sparrow and J. L. Gregg, A boundary-layer treatment of laminar film condensation, *J. Heat Transfer* **81,** 13–18 (1959).
4. J. C. Y. Koh, E. M. Sparrow and J. P. Hartnett, The two-phase boundary layer in laminar film condensation. *Int. J. Heat Mass Transfer* **2,** 69–82 (1961).
5. E. M. Sparrow and R. D. Cess, Free convection with blowing or suction, *J. Heat Transfer* **83,** 387–389 (1961).
6. J. T. Hong, C.-L. Tien and M. Kaviany, Non-Darcian effect on vertical-plate natural convection in porous media with high porosities, *Int. J. Heat Mass Transfer* **28,** 2149–2157 (1985).
7. W. G. Gray, General conservation equations for multi-phase systems: 4, constitutive theory including phase change, *Adv. Water Resources* **6,** 130–140 (1983).